

UNCLASSIFIED

AD 273 973

*Reproduced
by the*

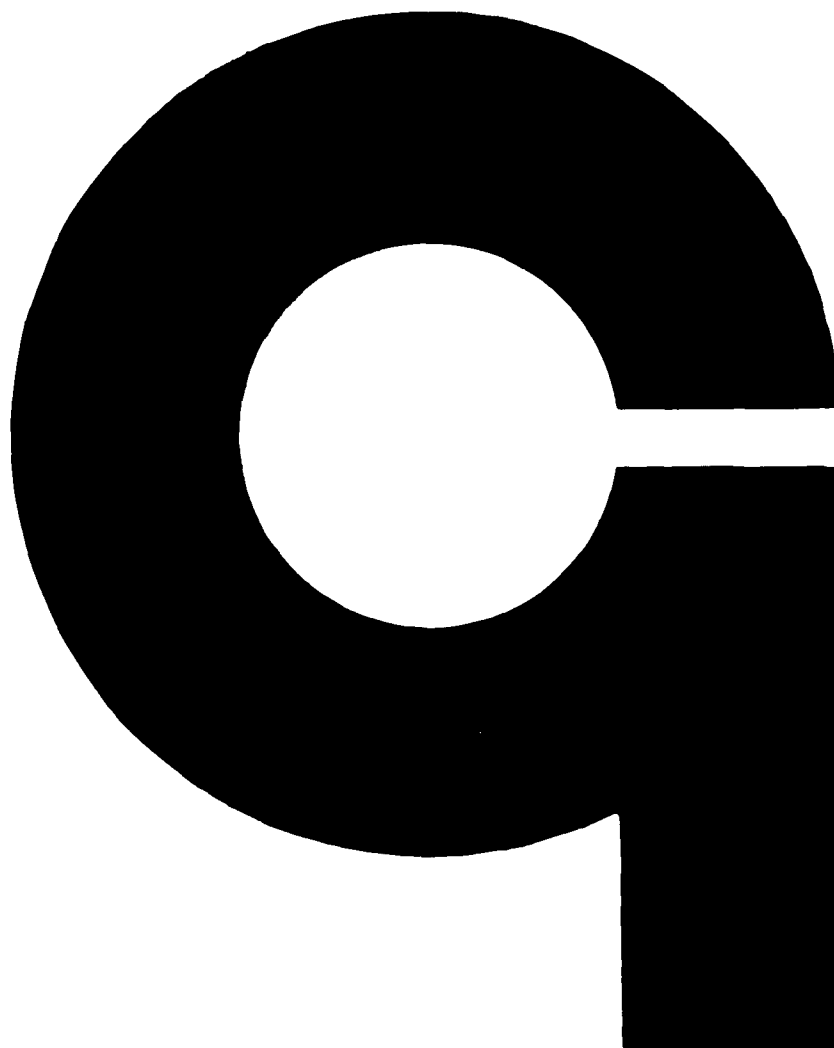
**ARMED SERVICES TECHNICAL INFORMATION AGENCY
ARLINGTON HALL STATION
ARLINGTON 12, VIRGINIA**



UNCLASSIFIED

NOTICE: When government or other drawings, specifications or other data are used for any purpose other than in connection with a definitely related government procurement operation, the U. S. Government thereby incurs no responsibility, nor any obligation whatsoever; and the fact that the Government may have formulated, furnished, or in any way supplied the said drawings, specifications, or other data is not to be regarded by implication or otherwise as in any manner licensing the holder or any other person or corporation, or conveying any rights or permission to manufacture, use or sell any patented invention that may in any way be related thereto.

273973



STEADYSTATE ELECTRON DENSITIES FOR IRRADIATED PLASMAS

BY

J. I. F. KING AND R. SILLARS

QUARTERLY TECHNICAL NOTE

CONTRACT NO. AF 30(602)-2380

PREPARED FOR
ROME AIR DEVELOPMENT CENTER
AIR FORCE SYSTEMS COMMAND
GRIFFISS AIR FORCE BASE
NEW YORK

MARCH 1962

GEOPHYSICS CORPORATION OF AMERICA BEDFORD, MASSACHUSETTS

RADC TDR-62-106

STEADYSTATE ELECTRON DENSITIES
FOR IRRADIATED PLASMAS

J. I. F. King
R. Sillars

QUARTERLY TECHNICAL NOTE
Contract No. AF 30(602)-2380
Project No. 5561
Task No. 55209
GCA Technical Report No. 62-8-A

March 1962

GEOPHYSICS CORPORATION OF AMERICA
Bedford, Massachusetts

Prepared for
Air Force Systems Command
Rome Air Development Center
Griffiss Air Force Base, New York

TABLE OF CONTENTS

<u>Section</u>	<u>Title</u>	<u>Page</u>
	ABSTRACT	1
I	INTRODUCTION	2
II	THEORY	4
III	CONCLUSIONS	24
	REFERENCES	25

STEADYSTATE ELECTRON DENSITIES FOR IRRADIATED PLASMAS

ABSTRACT

Steadystate electron density profiles have been calculated for diffusion- and recombination-controlled plasmas irradiated by an external source of electromagnetic flux. In the former case the internal electron generation caused by progressive beam absorption is balanced by electron diffusion across the plasma boundaries. In the second model the beam-stimulated electron growth is limited by recombination.

(U)

The efficiency of electron diffusion and consequent wall recombination as a heat transfer process is calculated and found never to exceed 30%. Furthermore, the nonlinear diffusion model gives rise to a stability criterion below which no steadystate electron configuration is possible.

(U)

I. INTRODUCTION

Previous reports^(1,2) have dealt in detail with the Dynamic Shield Response (DSR) of a slightly ionized plasma when subjected to electromagnetic radiation. The general features of the interaction are:

(1) a strong, initial thermal coupling just anterior to the resonant plasma frequency depth,

(2) a local increase in electron density coincident with the heat deposition which in turn affects the pattern of radiation attenuation, and

(3) a consequent upstream movement of an ionization front resulting from the electron growth which inhibits deep plasma penetration of the impressed radiation.

(U)

These DSR characteristics are displayed in Figure 1 for a nonuniform plasma with an initial exponential electron density distribution.

(U)

Models previously treated considered only electron growth effects, i.e., all relaxation mechanisms such as diffusion, recombination, and radiation were neglected. In this report the influence of diffusion in altering the electron density profile will be considered. Passing reference will be given to recombination and a time-dependent growth limiting process as well.

(U)

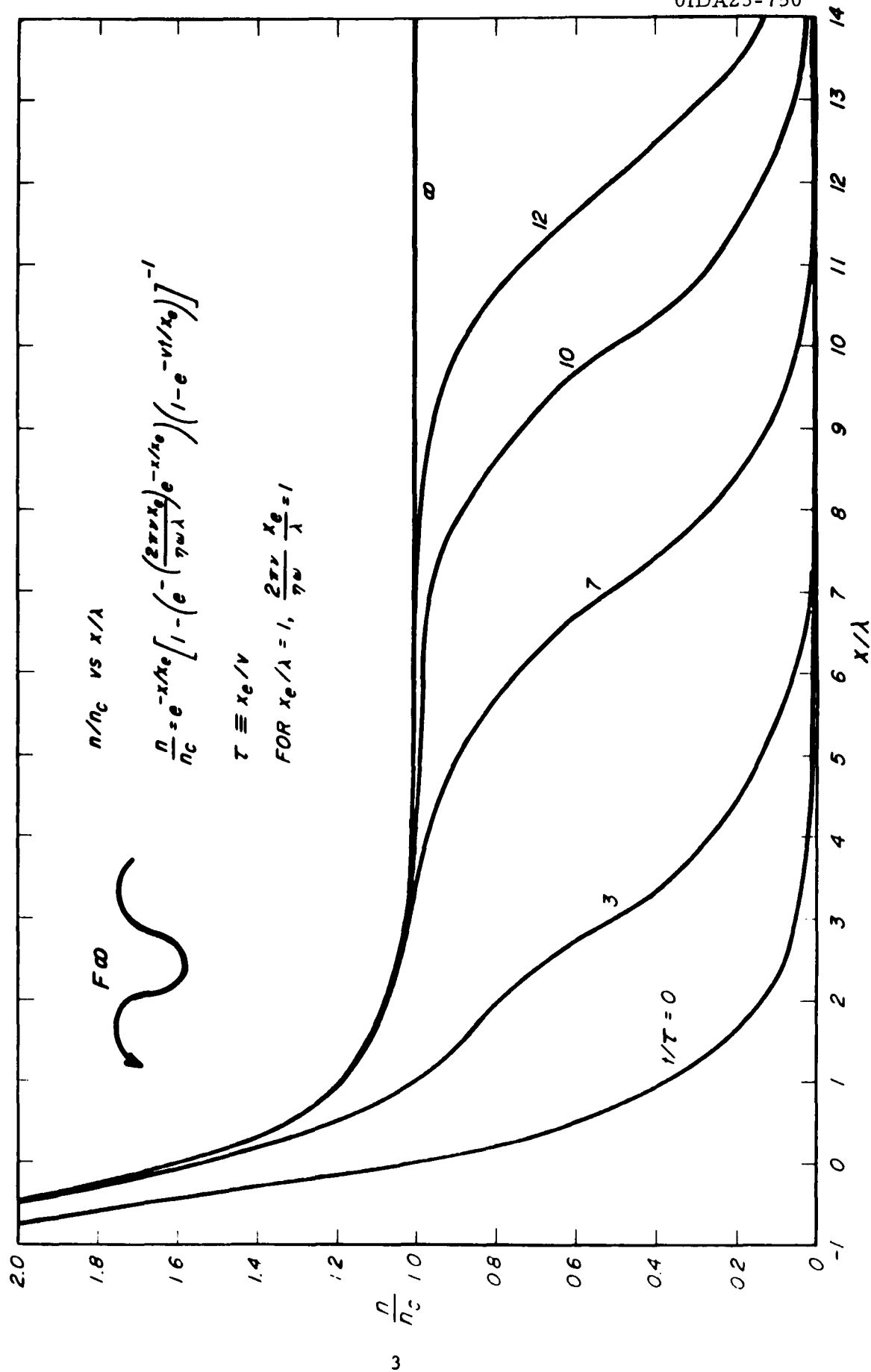


Figure 1. Time Response of the Electron Density of an Irradiated Plasma.

II. THEORY

By analogy with heat flow, we may add to the fundamental electron growth equation a diffusion term proportional to the divergence of the electron density gradient. Thus in our onedimensional model we have

$$\frac{\partial n}{\partial t} = \frac{f}{\epsilon} \sigma E^2 + D \frac{\partial^2 n}{\partial x^2} \quad (1)$$

where n is the electron density

f is the ionizing collision probability

ϵ is the molecule ionization energy

σE^2 is the electromagnetic flux extinction

D is the diffusion coefficient.

(U)

In this first order treatment we assume the diffusion coefficient is constant, leaving its exact magnitude unspecified.

(U)

We seek steadystate solutions of Equation (1) which, of course, implies that $\partial n / \partial t = 0$. This simplifies the hyperbolic partial differential equation into an elliptic type involving only one independent variable

$$\frac{d^2 n}{dx^2} = - \frac{f}{\epsilon D} \sigma E^2 \quad (2)$$

(U)

In our model electrons are generated at varying rates inside the plasma. The solutions of Equation (2) will give us those configurations for which the outward diffusion of electrons at the boundaries exactly balances their internal growth.

(U)

Unfortunately, the steadystate assumption implies equilibrium and thus says nothing about the time taken to approach equilibrium. This would involve a complete solution of Equation (1). However, some appreciation of the magnitude of the growth constant may be gained from earlier nondiffusion work⁽²⁾ where the time constant τ was shown to be

$$\tau^{-1} = \frac{fF_{\infty}}{en_c} \frac{2\pi}{\eta\lambda} \frac{\nu}{\omega} \quad (3)$$

where: F_{∞} is the flux incident from large x

$n_c = (\epsilon_0 m/e^2)(\omega^2 + \nu^2)$ is the critical electron density

e, m are the charge and mass of the electron

$\eta = \sqrt{(\epsilon/\epsilon_0)}$ is the index of refraction, the squareroot of the ratio of the dielectric constant of the medium and free space

λ, ω are the in vacuo wavelength and radian frequency of the electromagnetic radiation

ν is the collision frequency of the electrons with the numerically preponderant neutral molecule background.

(U)

We take for our model an infinite plasma slab of thickness ℓ . The electron densities at the boundaries 0 and ℓ are to be kept at zero. This corresponds to infinite sinks for the electrons diffusing to the boundaries. A monochromatic, steady flux F_0 of frequency ω is incident from left to right on the slab as indicated in Figure 2.

(U)

As in the previous work we assume the plasma absorbs and transmits, but does not reflect. This enables us to use the WKB approximation which transforms Equation (2) to

$$\frac{d^2 n}{dx^2} = - \frac{f F_0}{e D} \kappa \exp \left(- \int_0^x \kappa dx \right) \quad (4)$$

where $\kappa = \frac{2\pi}{\eta \lambda} \frac{\nu}{\omega} \frac{n}{n_c}$ is the absorption coefficient, a linear function of

electron density in this approximation.

(U)

Multiplication by the factor κ/n simplifies Equation (4) to

$$\frac{d^2 \kappa}{dx^2} = - \frac{\kappa}{A} \exp \left(- \int_0^x \kappa dx \right), \quad (5)$$

$$\frac{1}{A} = \frac{f F_0}{e n_c D} \frac{2\pi}{\eta \lambda} \frac{\nu}{\omega}$$

where A is a constant having the dimensions of L^2 .

(U)

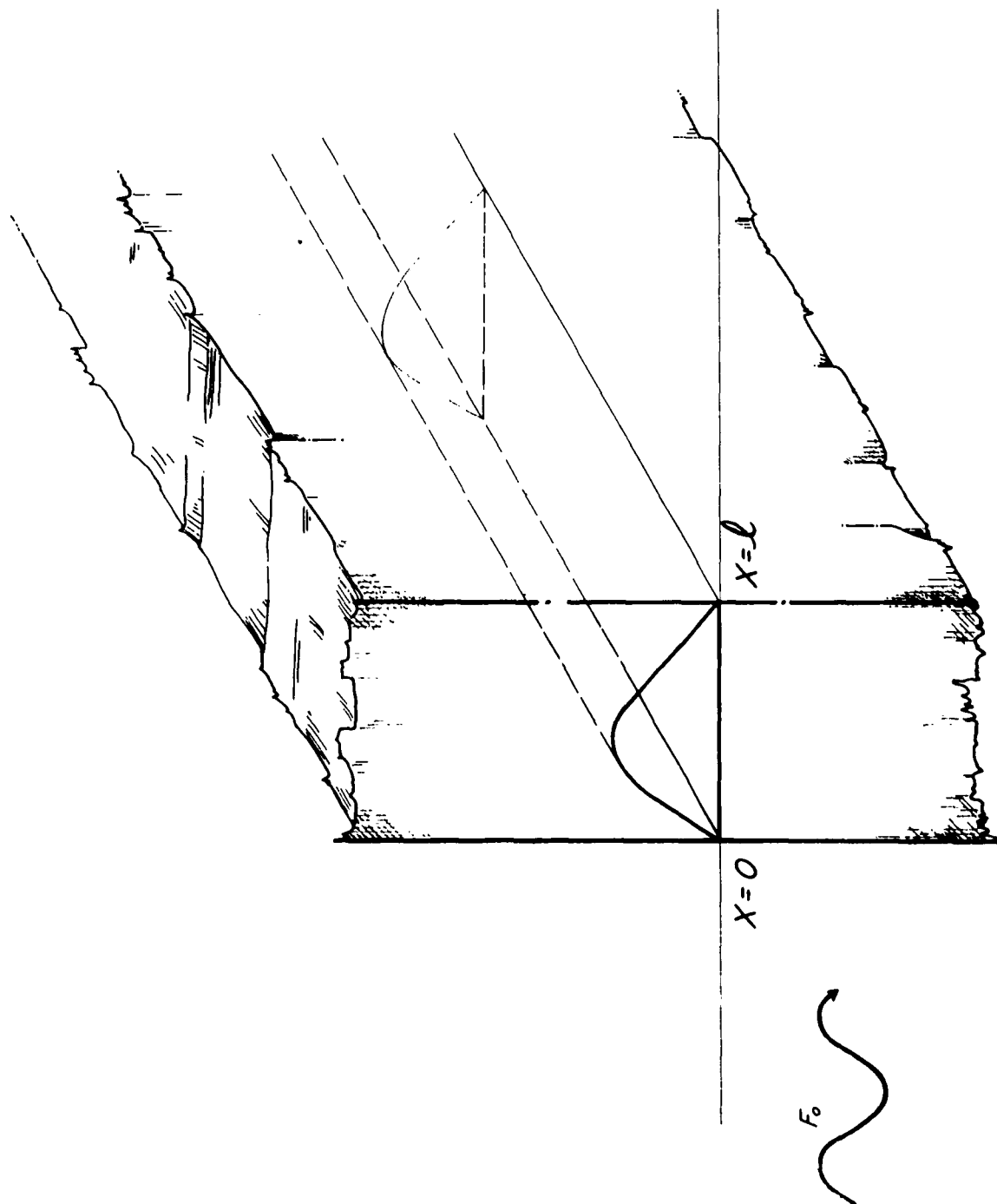


Figure 2. Schematic Model of Diffusion Equilibrium Electron Density Profile.

Our task then is the solution of the integrodifferential Equation (5) yielding the absorption coefficient (and hence the equilibrium electron density) as a function of position for various plasma models.

(U)

We begin with the optical depth substitution

$$\xi = \int_0^x \kappa \, dx$$

which eliminates the integral but increases the order of Equation (5).

Thus

$$\frac{d^3 \xi}{dx^3} = - \frac{\exp(-\xi)}{A} \frac{d\xi}{dx} \quad (6)$$

(U)

This equation integrates at once to

$$\frac{d^2 \xi}{dx^2} = \frac{\exp(-\xi) - \exp(-\xi_m)}{A} \quad (7)$$

where the constant ξ_m is the value of ξ for which $\kappa = \kappa_{\max}$, i.e., $(d\kappa/dx) =$

$$(d^2 \xi / dx^2) = 0.$$

(U)

The integrating factor $2d\xi/dx$ enables us to perform the second integration

$$\frac{2d\xi}{dx} \frac{d^2\xi}{dx^2} = \frac{d}{dx} \left(\frac{d\xi}{dx} \right)^2 = \frac{2}{A} [\exp(-\xi) - \exp(-\xi_m)] \frac{d\xi}{dx}$$

(U)

This leads immediately to

$$\kappa^2 = \left(\frac{d\xi}{dx} \right)^2 = \frac{2}{A} [1 - \exp(-\xi) - \xi \exp(-\xi_m)] \quad (8)$$

where we have determined the constant of integration by requiring that

$\kappa = (d\xi/dx) = 0$ at the boundary $\xi = 0$.

(U)

Equation (8) expresses the absorption coefficient as a function of the optical depth. This is not the form we want. We wish to express κ as a function of position. Before continuing, we note that the imposition of the second boundary condition $\kappa = 0$ at $\xi = \xi_\ell$, where ξ_ℓ is the total optical thickness of the plasma, serves to determine ξ_ℓ as a function of ξ_m . Thus, from Equation (8) at $x = \ell$ we must have

$$1 - \exp(-\xi_\ell) - \xi_\ell \exp(-\xi_m) = 0 \quad (9)$$

The solution of this transcendental equation which we shall require presently is plotted in Figure 3.

(U)

Returning to the main problem, both the absorption coefficient and position can be expressed as parametric functions of the optical depth.

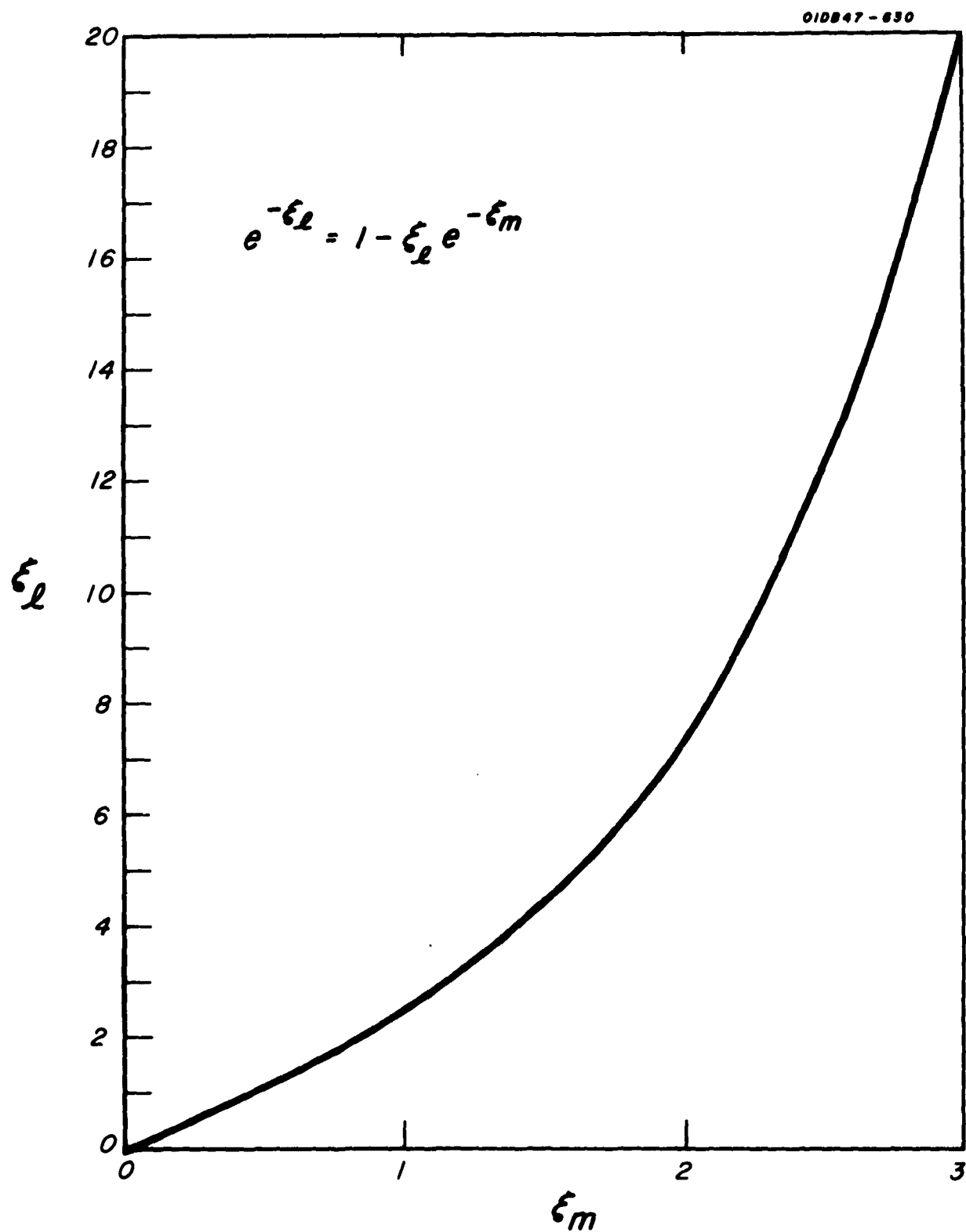


Figure 3. Total Optical Depth vs. Optical Depth at Maximum Electron Density.

From the definition of the optical depth we have

$$dx = \frac{d\xi}{\kappa} , \quad x = \int_0^{\xi} \frac{d\xi}{\kappa(\xi)} , \quad \ell = \int_0^{\xi_\ell} \frac{d\xi}{\kappa(\xi)}$$

where ℓ is the plasma thickness.

(U)

By using Equation (8) and Figure 3, we obtain the definite integral relating the plasma thickness to the total optical depth of the plasma

$$\ell \sqrt{\frac{2}{A}} = \int_0^{\xi_\ell} [1 - \exp(-\xi) - \xi \exp(-\xi_m)]^{-1/2} d\xi \quad (10)$$

This quadrature has been performed numerically and is displayed in Figure 4. Although the integrand diverges as ξ approaches 0 and ξ_ℓ , simple analysis shows that the integral remains finite. By appropriate expansions of the integrand the following limiting values can be found:

$$\ell \sqrt{\frac{2}{A}} = \pi \sqrt{2} \quad \text{for } \xi_\ell \ll 1,$$

$$\ell \sqrt{\frac{2}{A}} = 2\xi_\ell + 2 \ln 2 \quad \text{for } \xi_\ell \gg 1.$$

Note the interesting result that $\ell \sqrt{(2/A)}$ remains finite as ξ_ℓ approaches zero.

(U)

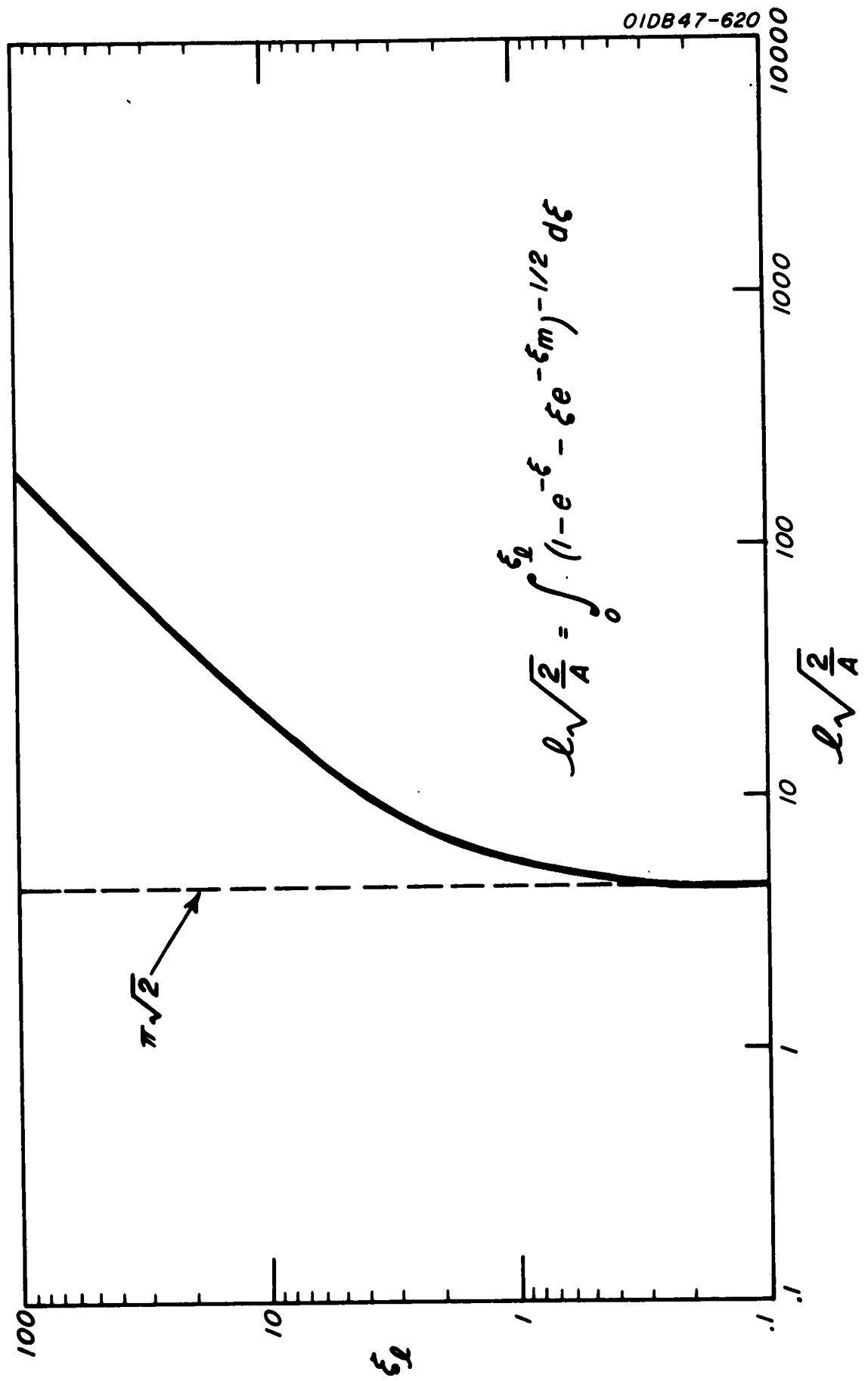


Figure 4. Total Optical Depth vs. Grouped Plasma Parameters.

Finally, in Figure 5 we have plots of the absorption coefficient (electron density) against position for various fixed values of the plasma parameters. The ordinate is obtained from the relation

$$\kappa \sqrt{\frac{A}{2}} = [1 - \exp(-\xi) - \xi \exp(-\xi_m)]^{1/2}$$

while the corresponding abscissa follows by numerical integration from

$$\frac{\xi}{\ell} = \frac{\int_0^{\xi} [1 - \exp(-\xi) - \xi \exp(-\xi_m)]^{-1/2} d\xi}{\int_0^{\xi_\ell} [1 - \exp(-\xi) - \xi \exp(-\xi_m)]^{-1/2} d\xi}$$

(U)

Our theory for the diffusion model is now complete for, given a plasma thickness ℓ and the value of the lumped parameters, A , we can uniquely specify the equilibrium electron density distribution. From Figure 5 we note that the equilibrium density is symmetric about the midpoint for small total optical thickness ξ_ℓ , or equivalently, for low values of $\ell \sqrt{(2/A)}$. As, for example, the incident flux F_0 increases, the equilibrium optical depth grows as well with the profile becoming skewed toward the incoming beam. The steeper slope adjacent to the incident flux increases the electron diffusion out at this boundary relative to the diffusion at the opposite surface.

(U)

Thus, qualitatively, by increasing the electromagnetic flux we augment the diffusion at the outer boundary with little effect in the

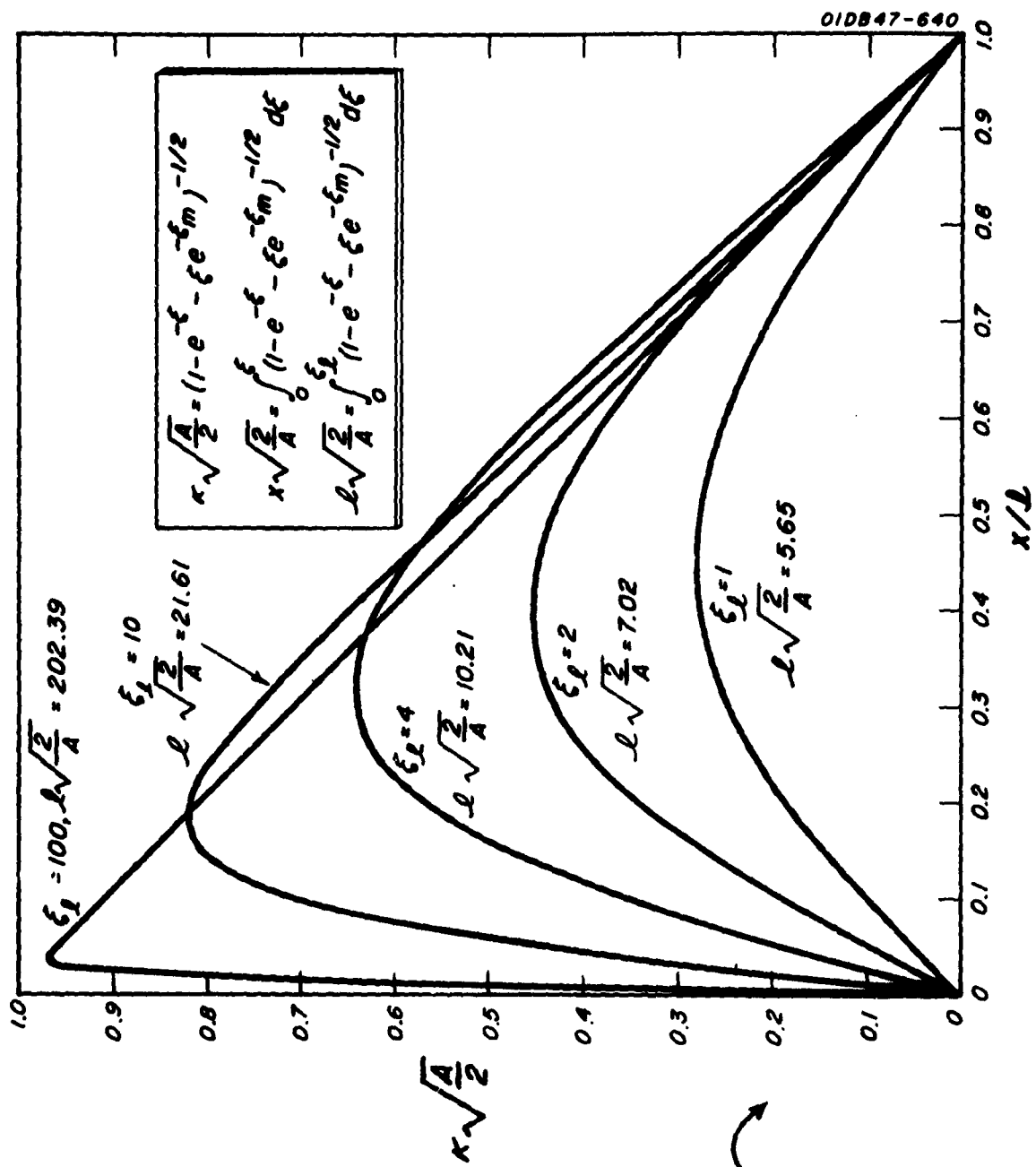


Figure 5. Diffusion Equilibrium Electron Density Profiles.

plasma interior. Thus the nonlinear plasma response tends to thwart efforts to alter inner transport behavior.

(U)

These conclusions are rendered more quantitative by considering the efficiency of electron diffusion as an energy transfer mechanism. We will assume that the electrons reaching the inner surface at $x = \ell$ recombine, yielding up all their ionization energy in the process. The ratio of electrons reaching the interior boundary to all those being created in the plasma is, from Equation (7)

$$\frac{|dk/dx|_{x=\ell}}{|dk/dx|_{x=0}} = \frac{\exp(-\xi_m) - \exp(-\xi_\ell)}{1 - \exp(-\xi_\ell)} \quad (11)$$

(U)

On the other hand the fraction of the incident flux going into the production of electrons is

$$\begin{aligned} \frac{f \int_0^\ell \sigma E^2 dx}{F_0} &= f \int_0^\ell \kappa \exp\left(-\int_0^x \kappa dx\right) dx = f \int_0^{\xi_\ell} \exp(-\xi) d\xi \\ &= f[1 - \exp(-\xi_\ell)] \end{aligned} \quad (12)$$

(U)

The efficiency is the ratio of the heating rate of inner wall recombination to the incident flux and is given by the product of Equations (11) and (12)

$$\text{eff} = f[\exp(-\xi_m) - \exp(-\xi_\ell)] \quad (13)$$

(U)

The ionizing collision probability f is, of course, less than unity and for electron temperatures of several electron volts is of the order of 0.1⁽²⁾. Figure 6 is a plot of the efficiency as a function of equilibrium total optical thickness. The maximum attainable efficiency for $f = 1$ is 30% and occurs at $\xi_\ell = 1.79$. For large optical thicknesses the efficiency drops off inversely with ξ_ℓ leading to

$$\text{eff} = \frac{f}{\xi_\ell} = \frac{f \sqrt{(2A)}}{\ell}, \quad \xi_\ell \gg 1$$

(U)

As the total power F_o is increased the total energy transferred through wall recombination increases as the square-root of F_o , a result which follows from the expression for A . Thus

$$\dot{Q}_w = \frac{fF_o}{\xi_\ell} = \text{const} (fF_o)^{1/2} \quad (14)$$

where \dot{Q}_w is the wall heating rate.

(U)

This conclusion most certainly overestimates the rate of increase of wall transfer with higher flux because of the neglect of reflection. From Equation (7) we see that the slope of the density profile at the outer boundary increases linearly with the incident flux

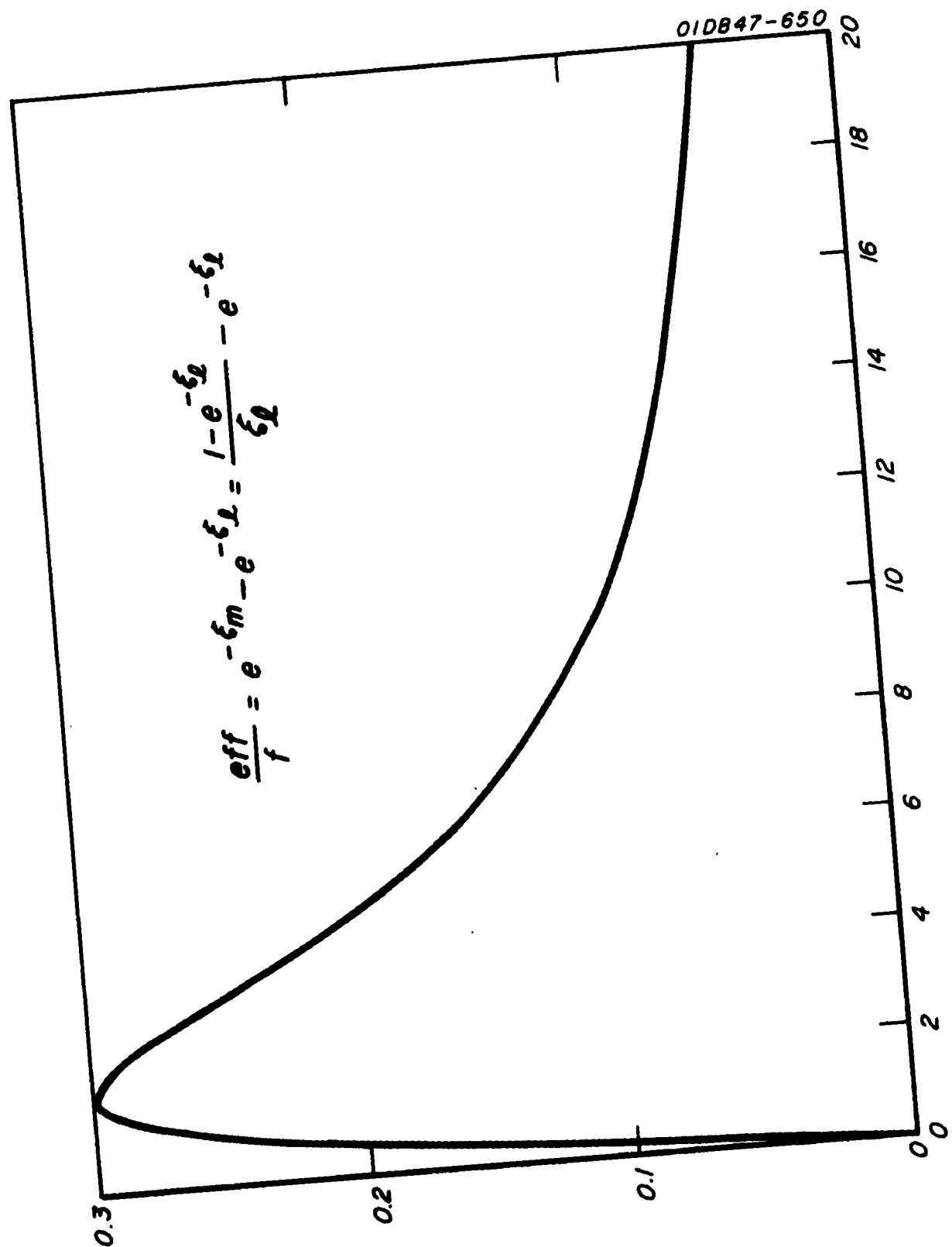


Figure 6. Efficiency vs. Equilibrium Total Optical Depth.

$$\left. \frac{dK}{dx} \right|_{x=0} = \frac{1 - \exp(-\xi_m)}{A} \approx \frac{1}{A}, \text{ for } \xi_\ell \gg 1 \quad (15)$$

(U)

The discontinuity in slope at the boundary will tend to reflect the incident beam with increasing effectiveness for increasing flux. This will temper the growth factor in Equation (14), so that the squareroot wall transfer dependence on the flux should be viewed as an upper limit.

(U)

One unexpected effect merits discussion. This is the fact that (see Figure 4) the nondimensional parameter $\ell \sqrt{2/A}$ approaches the finite value $\pi \sqrt{2}$ as the equilibrium optical depth ξ_ℓ tends towards zero. Physically this implies that there are no stable equilibrium configurations when the following lumped plasma parameters are less than unity

$$\frac{\ell^2 f F_0}{\pi^2 e n_c D} \frac{2\pi \nu}{\eta \lambda \omega} < 1 \quad (16)$$

(U)

Let us imagine a plasma being irradiated with an increasingly intense beam. Since the ionizing collision probability is a monotonic function of electron temperature and hence of incident flux, there will always be a power range satisfying this inequality. Wall transfer at this flux intensity would therefore occur only in some unstable, unsteady fashion. We are forced to conclude that no steady diffusion

pattern can be established until the power level determined by the inequality is exceeded.

(U)

We turn now to treat another electron relaxation mechanism, viz., recombination within the plasma. The fundamental equation in this case, neglecting now diffusion, becomes

$$\frac{\partial n}{\partial t} = \frac{f}{e} \sigma E^2 - \beta n^2 \quad (17)$$

We have assumed the recombination rate is equal to the product of a generalized coefficient β and the square of the electron density, reflecting the fact that deionization must involve collisions between charged particles.

(U)

The steadystate configurations are then the solutions of the equation

$$n^2 = \frac{f F_0}{e \beta} \kappa \exp \left(- \int_0^x \kappa \, dx \right) \quad (18)$$

(U)

By making use of the proportionality of the absorption coefficient and electron density, we can transform this equation to

$$\kappa = \kappa_0 \exp \left(- \int_0^x \kappa \, dx \right) \quad (19)$$

where

$$\kappa_o = \left(\frac{2\pi}{\eta\lambda} \frac{\nu}{n_c} \right)^2 \frac{fF_o}{r\beta}$$

is the value of the absorption coefficient at the outer boundary $x = 0$.

(U)

Using elementary analysis we readily find as solutions of Equation (19) the family of hyperbolas

$$\kappa = \frac{\kappa_o}{\kappa_o x + 1} \quad (20)$$

(U)

Figure 7 is a universal plot of these recombination-controlled equilibrium electron density configurations. Once again since the beam interaction is strongest at the outer boundary we find an electron maximum there having the finite value

$$n_o = \frac{fF_o}{en_c\beta} \frac{2\pi}{\eta\lambda} \frac{\nu}{\omega} \quad (21)$$

This maximum electron density is, among other things, directly proportional to the electromagnetic flux.

(U)

As a final model we treat a time-dependent electron profile growth which perhaps logically belongs in a previous report⁽²⁾. Ignoring all

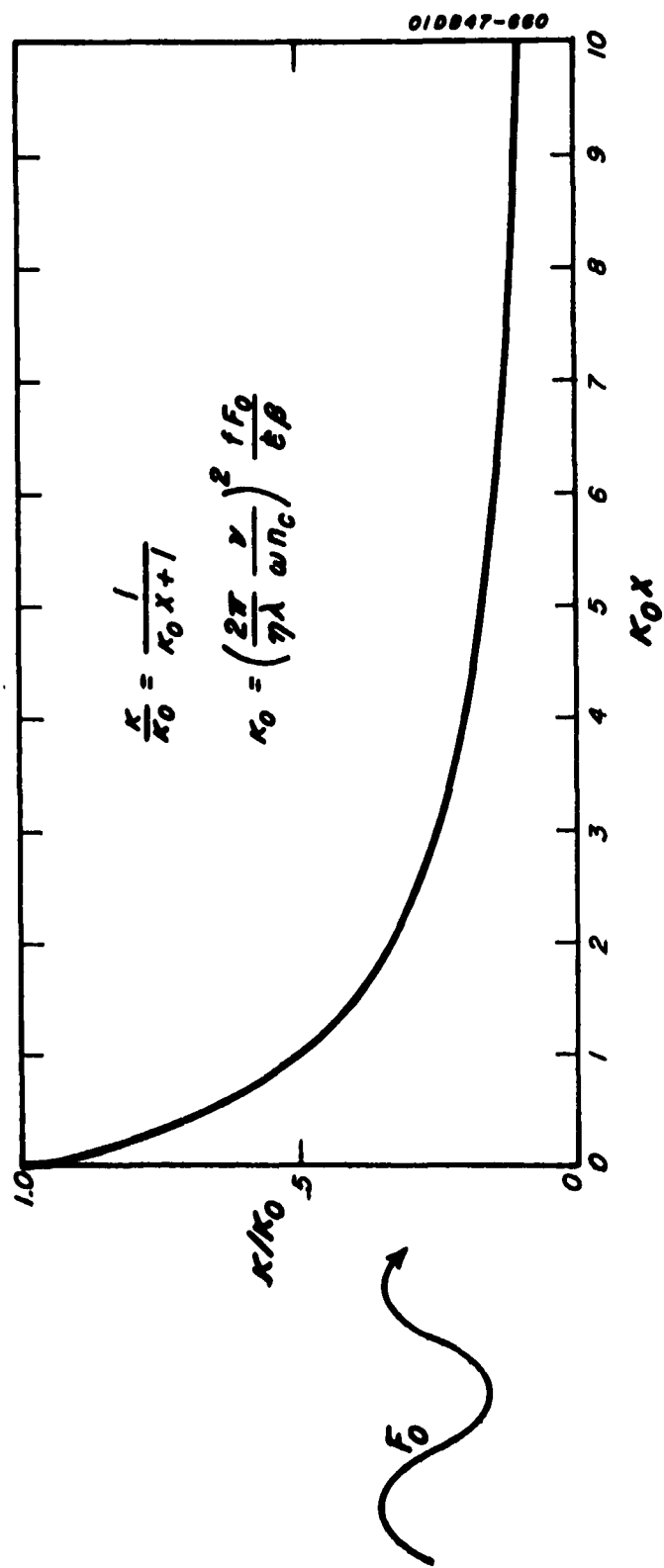


Figure 7. Recombination Equilibrium Electron Density Profile.

relaxation effects, the fundamental growth equation can be written, say for our infinite sink model irradiated in the positive x-direction

$$\frac{\partial n}{\partial t} = \frac{f}{e} \sigma E^2 = \frac{f}{e} F_0 \kappa \exp \left(- \int_0^x \kappa \, dx \right) \quad (22)$$

(U)

Strictly speaking this equation is invalid since it predicts, for example at the outer boundary an unlimited exponential growth of electron density. The correct form includes a factor which accounts for the fact that the probability of an ionizing collision decreases as the medium becomes ionized. Thus we can more correctly write the growth equation as

$$\frac{\partial \kappa}{\partial t} = \frac{\kappa}{\tau} \left(1 - \frac{n}{N} \right) \exp \left(- \int_0^x \kappa \, dx \right) \quad (23)$$

where N is the number density of neutral molecules and positive ions (assumed singly ionized).

(U)

A closed form solution of Equation (23) appears impossible to obtain. The solution at the outer boundary, however, follows readily by elementary integration

$$n = \frac{N}{[1 + \exp(-t/\tau)] \left(\frac{N}{n_0} - 1 \right)} \quad (24)$$

where n_0 is the initial electron density at $x = 0$. Thus the plasma at the boundary approaches asymptotically with time the finite, completely-ionized density $n = N$.

(U)

III. CONCLUSIONS

The steadystate electron distribution has been calculated for a confined plasma in which the internal electron generation is balanced by diffusion across the boundaries. The profile is asymmetric with the steeper slope at the outer boundary where the radiation makes contact with the plasma. An increase in the flux density increases the equilibrium total optical depth, steepening the slope at the outer boundary but causing little change at the interior surface. The efficiency of wall recombination as an energy transfer process can never exceed 30%. At best, ignoring reflection, the wall heating rate cannot rise faster than the squareroot of the incident flux. If the product of the plasma thickness, ionizing collision probability, and incident flux falls below a certain critical value, no steadystate electron configuration is possible and the profile becomes unstable.

(U)

For a plasma in which the electrons are internally formed through impact ionization and lost through recombination, the equilibrium profile is hyperbolic. The electron density has its finite maximum at the outer plasma boundary trailing monotonically downward with deeper plasma penetration.

(U)

REFERENCES

1. King, J. I. F., "Steadystate Shielding Response of an Irradiated Plasma", GCA Technical Report 61-29-A, Contract No. AF 30(602)-2380, USAF, Rome, N.Y. (1961).
2. King, J. I. F., "The Dynamic Shielding Response of an Irradiated Plasma, I", GCA Technical Report 62-5-A, Contract No. AF 30(602)-2380, USAF, Rome, N.Y. (1962).